Mahendra S. Gaikwad* and Chandrajit Balomajumder

TFC polyamide NF membrane: characterization, application and evaluation of MTPs and MTC for simultaneous removal of hexavalent chromium and fluoride

DOI 10.1515/epoly-2016-0219
Received August 5, 2016; accepted September 24, 2016; previously published online October 20, 2016

Abstract: The aim of the present work was check the feasibility of thin film composite (TFC) polyamide NF500 nanofiltration (NF) membrane for simultaneous removal of hexavalent chromium [Cr(VI)] and fluoride from a synthetically prepared binary solution. The characterizations of the membrane were made with techniques like Fourier transform infrared (FTIR) spectroscopy, scanning electron microscopy (SEM) and atomic force microscopy (AFM). The study of simultaneous removal of Cr(VI) and fluoride ions at different parameters such as feed concentration, pressure and pH. Evaluation of mass transfer coefficient (MTC) and membrane transport parameters (MTPs) using the combined film theory-Spiegler-Kedem (CFSK) model. The estimated parameters are used to predict membrane performance for simultaneous removal of Cr(VI) and fluoride. Experimental results and model predicted results that show good correlations.

Keywords: fluoride; hexavalent chromium; nanofiltration; NF500 membrane; polyamide.

1 Introduction

Recently application of the nanofiltration (NF) has been enhanced in the field of desalination, chemical, biotech, petrochemical industries as the NF process overcomes operational difficulties that are related with conventional processes. Many studies are reported on heavy metals and metals ions removal by NF (1–4). Industries like leather, dye, electroplating, textiles and the discharge of such industries use chromium salts and produce high levels of chromium in different forms (trivalent and hexavalent chromium) in their waste stream (5). Generally hexavalent chromium [Cr(VI)] is more toxic than trivalent chromium [Cr(III)]. It is harmful and effects the skin, kidneys, respiratory tract and develops genetic deformation by DNA destruction (6). Thus there is need to remove such highly toxic ions before discharge to the environment. Various technologies are reported for the elimination of Cr(VI) from water such as precipitation (7), ion-exchange (8), adsorption (9–11) and membrane-based separation (12–14). On the other hand, fluoride has also been found in the wastewater discharge of metal processing, glass manufacturing, semiconductor and fertilizer industries (15–19). Fluoride concentration range 0.5–1.5 mg/l in water is useful for human health up to a limit but concentrations beyond 1.5 mg/l creates problems like dental/skeletal fluorosis, neurotransmitters, fetal cerebral function and many other illnesses (20–22). Different techniques were reported for the elimination of fluoride such as precipitation (23), ion exchange (24), electrodialysis (25), adsorption (26–29) and membrane separation (30, 31). In semiconductor industries mainly in wafer manufacturing numerous types of chemicals are applied (32, 33). Fluoride, heavy metals, toxic solvent different salts and chelating agents may be found in wastewater discharge of the semiconductor manufacturing industry (33). Wafer surface etching processes produce some waste-like chromic acids, sulfuric, hydrochloric, phosphoric, nitric, hydrofluoric and chromic acids. Mainly HF/chromic acid are used in Secco and Yang etching processes (34, 35). Thus, the fluoride and Cr(VI)-like toxic ions are found in semiconductor effluents (36, 37). Thus simultaneous elimination of Cr(VI) and fluoride is necessary from wastewater. The aim of the current work is to study characterizations of NF500 membranes by Fourier transform infrared (FTIR) spectroscopy, scanning electron microscopy (SEM) and atomic force microscopy (ARM). Also to investigate the effect of various parameter such as pressure, feed concentration and pH of feed on simultaneous removal of Cr(VI) and fluoride from binary aqueous solutions by NF500 membrane. Evaluation of

***Corresponding author: Mahendra S. Gaikwad,** Department of Chemical Engineering, Indian Institute of Technology Roorkee, Roorkee-247667, Uttarakhand, India,
e-mail: mahendra14g@gmail.com
Chandrajit Balomajumder: Department of Chemical Engineering, Indian Institute of Technology Roorkee, Roorkee-247667, Uttarakhand, India

mass transfer coefficient (MTC) and membrane transport parameters (MTPs) are done using the combined film theory-Spiegler-Kedem (CFSK) model.

2 Materials and method

2.1 Chemicals and membranes

All the solutions are prepared with deionized (DI) water. The feed solution of Cr(VI) and fluoride was prepared with the required amounts of potassium dichromate ($K_2Cr_2O_7$) (SDFCL, Mumbai, India) and sodium fluoride (NaF) (SDFCL, Mumbai, India) in DI water. A commercial NF500 membrane was procured from Permionics Membranes Pvt. Ltd. (Vadodara, India). Specifications of membrane are MWCO (500 Da), pH range (2–11), maximum temperature (40°C).

2.2 Experimental

The Perma® membrane system (Permionics Membranes Pvt. Ltd., Vadodara, India) was used for the experiment. Experiments were carried with a flat sheet membrane module having two housing plates for flat sheet membranes. The top plate was for flow channels and the bottom was used as a support with permeate passage. The schematic of the experimental set up is shown in Figure 1. A binary mixture of Cr(VI) and fluoride was treated with commercial NF500 NF membrane in a cross flow batch circulation mode. The effective surface area of the membrane was 25 cm^2. Initially the experiment setup was run for 1–2 h at 10 bar pressure with DI water for stabilization of membrane. The feed concentration of the binary solution of Cr(VI) and fluoride was maintained constant by continuous recycling outlets streams to the feed tank. The experiments were carried out with different pressure from 2 bar to 10 bar with various concentrations of feed solution ranging from 5 ppm to 100 ppm Cr(VI) and fluoride. The permeate flux (J_v, L/m^2 h) and the percent rejection of solute (%R_o) were measured. Calculation of the percent rejection of solute was carried out by using Eq. [1].

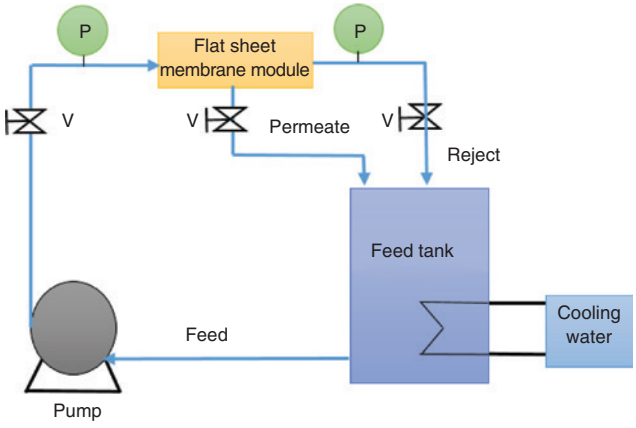

Figure 1: Schematic of experimental set up.

$$\%R_0 = \left[1 - \left(\frac{C_p}{C_f}\right)\right] \times 100 \quad [1]$$

where C_p and C_f signify the solute concentration in permeates and feed, respectively.

After each set of experiments, the set up was cleaned with DI water for 20–30 min at a pressure of 2 bar to gain the pure water permeability then next experiment was stared.

2.3 Characterization and analysis

Analysis of Cr(VI) and fluoride were carried out according to the standard diphenylcarbazide method (38) using a UV spectrophotometer (Hach DR-5000, HACH Co., USA). Fluoride analysis was done by using ion chromatography (Metrohm Compact IC, Switzerland). Morphological, surface roughness and chemical composition of the NF500 membrane were carried out with SEM (FE-SEM Quanta 200 FEG, FEI Company, USA), atomic force microscopy (AFM) (NT-MDT, NTEGRA, Russia) and FTIR spectroscopy (Perkin Elmer spectrum GX range spectroscopy, USA).

3 MTPs and MTC estimation

3.1 Film theory

Concentration of solute increases near the surface of the membrane due to rejection of the solute by the membrane. Thus the concentration build-up at the interface of membrane – liquid is called the concentration polarization. The material balance for the solute in a differential element as per film theory and applicable boundary conditions gives (39):

$$\left(\frac{C_{A2} - C_{A3}}{C_{A1} - C_{A3}}\right) = exp\left(\frac{J_v}{k}\right) \quad [2]$$

$$R_0 = \frac{(C_{A1} - C_{A3})}{C_{A1}} \quad [3]$$

$$R = \frac{(C_{A2} - C_{A3})}{C_{A2}} \quad [4]$$

Here

C_{A1}, C_{A2}, C_{A3}, J_V and k are the concentrations of solute in the feed, concentrations of solute in the boundary layer near the high-pressure side of the membrane, permeate concentrations of solute, permeate volume flux and MTC, respectively.

3.2 CFSK model

The CFSK model was the combined equation of the film theory and Spiegler-Kedem model (40). The CFSK model is used to evaluate MTC and MTPs simultaneously for a reverse osmosis system, which can also be used for NF (41–43).

The film theory equation can be arranged and written as

$$\left[\frac{R_0}{1-R_0}\right] = \left[\frac{R}{1-R}\right]\left[exp\left(\frac{-J_v}{k}\right)\right] \quad [5]$$

The nonlinear working equations of the Spiegler-Kedem model are as follows (39–42).

$$J_v = L_p(\Delta p - \sigma\Delta\pi) \quad [6]$$

$$R = \sigma[1 - exp(-J_v a_2)]/[1 - \sigma(exp(-J_v a_2))] \quad [7]$$

$$a_2 = \frac{(1-\sigma)}{P_m} \quad [8]$$

Eq. [3] can be rearrange in following form

$$\left[\frac{R}{1-R}\right] = a_1[1 - exp(-J_v a_2)] \quad [9]$$

$$a_1 = \frac{\sigma}{1-\sigma} \quad [10]$$

By putting Eq. [9] in to Eq. [5],

$$\left[\frac{R_0}{1-R_0}\right] = a_1[1 - exp(-J_v a_2)]\left[exp\left(\frac{-J_v}{k}\right)\right] \quad [11]$$

This is the equation of the CFSK model and it is used for the simultaneous evaluation of the MTC (k) and MTPs (σ and P_m) by providing the data of R_o and J_v with the help of a nonlinear parameter estimation method at different pressures and a constant feed rate by keeping the constant feed concentration.

4 Result and discussion

4.1 Investigation of pure water permeability (PWP) of the membrane

Before the starting of experiment the PWP of NF500 membrane was found by running DI water through the experimental set up. The PWP coefficient (L_p) value was found by plotting PWP versus applied pressure. The L_p value was the slope of that graph. The PWP coefficient was found to be 13.5 L/m²h bar for NF500 which was in the range of NF membranes (44, 45).

4.2 Characterizations of membranes

4.2.1 FTIR

Chemical composition and vibration details of the NF500 NF membrane was done by FTIR analysis (see Figure 2). A detailed description of the peaks in the FTIR graph are shown in Table 1.

4.2.2 SEM

The morphological structures of NF500 are obtained by using SEM. Figure 3A–F shows the top surface morphology and cross sectional view of the NF500 membrane at different magnification. The top surface of NF500 represents the

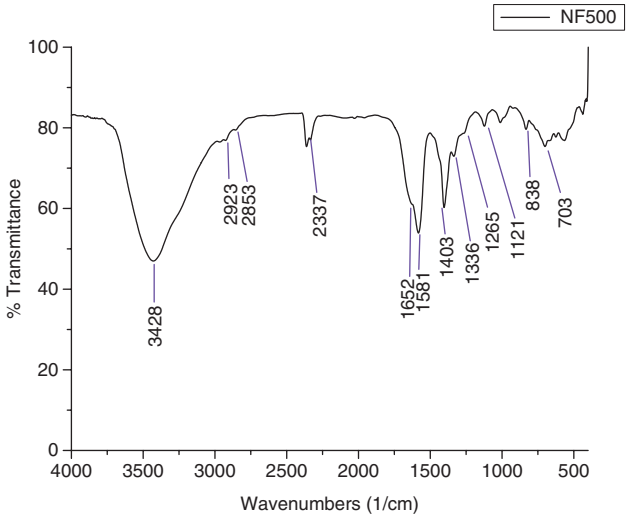

Figure 2: FTIR spectra of commercial NF500 membrane.

Table 1: FTIR analysis details of NF500 membrane.

Peak in FTIR graph	Vibration details	Chemical compositions details
3428 (1/cm)	N-H stretching	Weak amides, primary and secondary amines
2923 (1/cm)	CH_2 stretching	Anti-symmetric type aromatics
2853 (1/cm)	C-H stretching	Alkane compounds
2337 (1/cm)	C=N stretching	Nitrile group
1652 (1/cm)	C=O stretching	Secondary amide
1575 (1/cm)	C-C stretching vibration	Aromatic ring compound
1403 (1/cm)	OH bend stretching	–
1336 (1/cm), 1265 (1/cm), 1121 (1/cm)	C-O stretching	Presence of sulfonic group along
838 (1/cm), 703 (1/cm)	Aromatic C-H bending	Confirming polysulfone structure

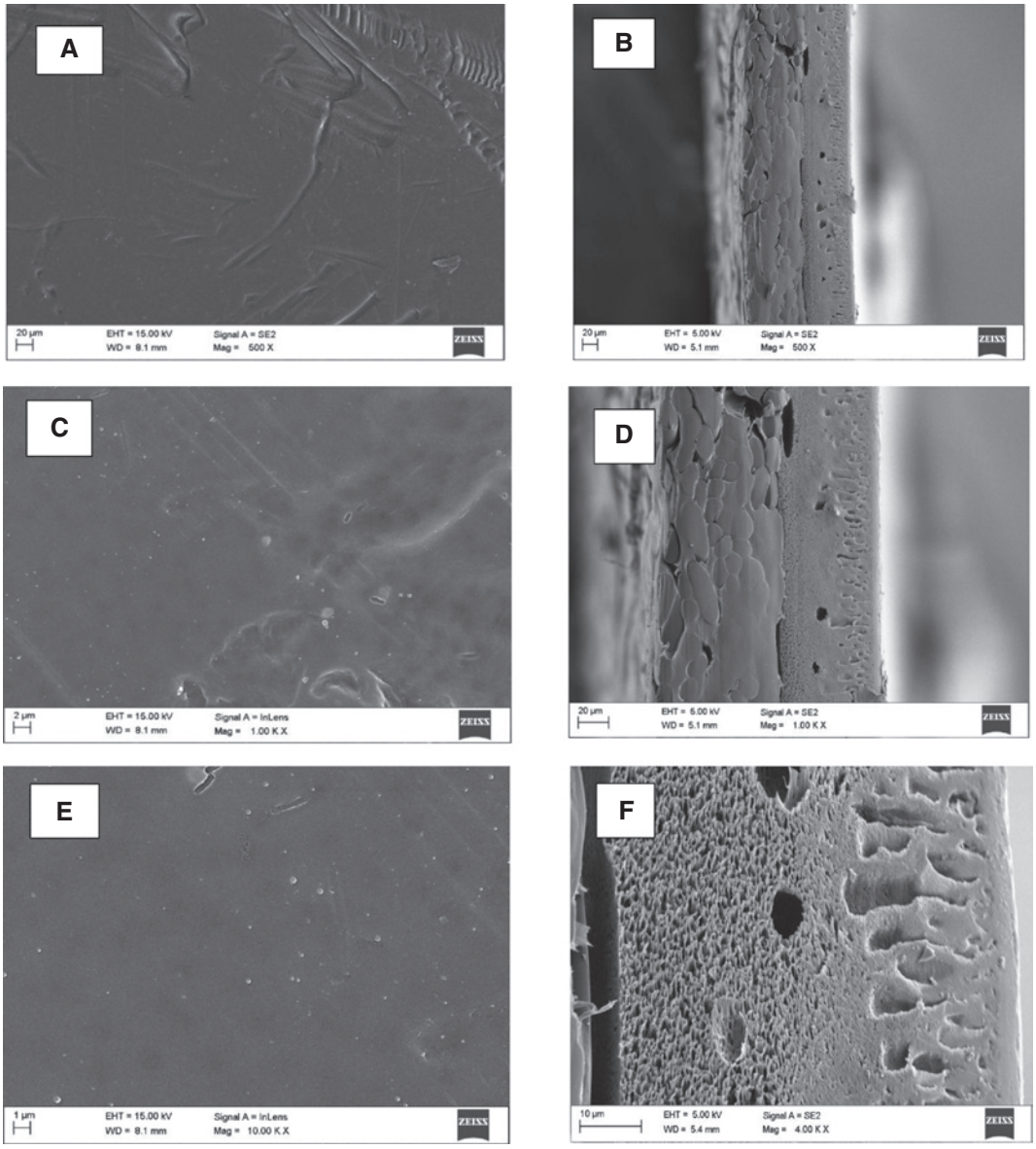

Figure 3: SEM image of commercial NF500 membrane (A) top view at 500 X (B) cross sectional view at 500 X (C) top view at 1.00 KX (D) cross sectional view at 1.00 KX (E) top view at 10.00 KX (F) cross sectional view at 4.00 KX.

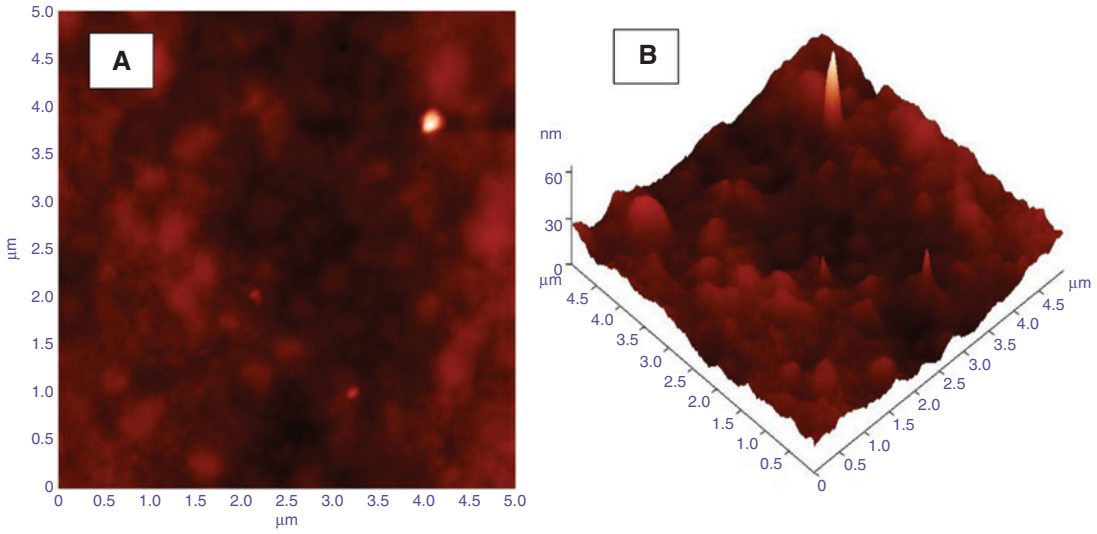

Figure 4: AFM image of commercial NF500 membrane (A) 2 D view (B) 3 D view.

asymmetric structure of the active layer of the polyamide polymeric material. The cross sectional view of the NF500 membrane clearly shows the composite of the three different layers of polymeric materials. The first layer is the polyamide polymer layer structure of that layer which has been shown at a higher magnification in Figure 3E, this is the active layer where the actual rejection of Cr(VI) and fluoride was done. The second layer and third layer consist of polysulfone and polyester, respectively.

4.2.3 AFM

Surface roughness and morphology was found with AFM. The two dimensional and three dimensional view of the surface of the NF500 membrane are clearly shown in Figure 4. The root mean square (RMS) roughness and average roughness values of NF500 were 4.82375 nm and 3.82525 nm by using NT-MDT SPM Software (Nova 1.0.26.1424, NT-MDT, Russia) of the selected area 5 µm × 5 µm of the membrane surface.

4.3 Pressure and feed concentration effect on rejection

The pressure and feed concentration effect on rejection of Cr(VI) and fluoride are shown in Figure 5. In the experiment the effect of the pressure study carried within a range of 2 bar to 10 bar and concentration of Cr(VI) and fluoride varies from 5 ppm to 100 ppm at a constant feed flow rate of 16 L/min. Figure 6 represent the effects pressure on the permeate flux of Cr(VI) and fluoride with the NF500 membrane.

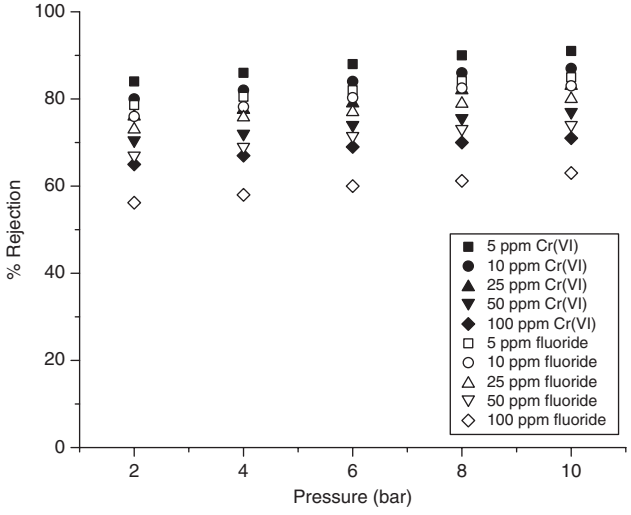

Figure 5: Effect of applied pressure on percentage rejection of Cr(VI) and fluoride with different feed concentration by using NF500 membrane at pH 8.

Figure 6 clearly shows that as the pressure increases then permeate flux linearly increases as represented by Eq. [6] which signifies that on the surface membrane, there is insignificant or no concentration polarization.

The solvent flux was enhanced without corresponding enhancement in the solute flux at increasing pressure due to solute and solvent flux separation in the solution-diffusion mechanism of NF membranes' transport mechanism (46). So the flux of pure water increases while there is no change or it remains in a constant flux of solute [Cr(VI) and fluoride] at increasing pressure because of this permeate contains less concentration of Cr(VI) and fluoride. This

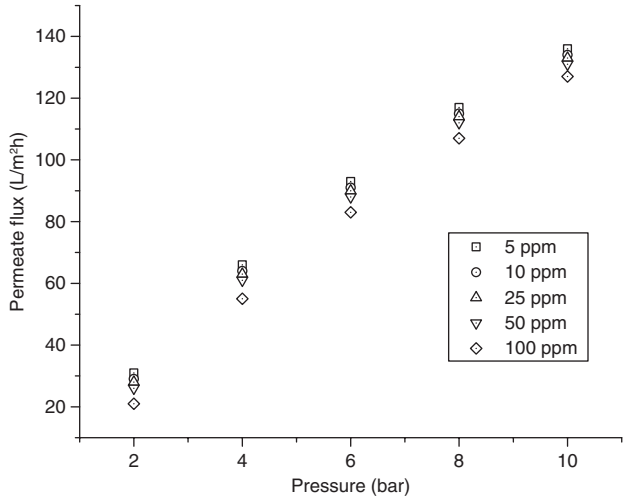

Figure 6: Effect of pressure on permeate flux of binary mixture of Cr(VI) and fluoride with different feed concentration by using the NF500 membrane.

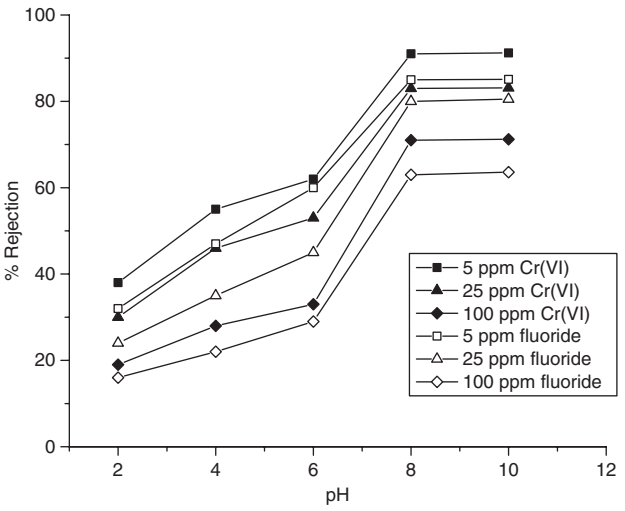

Figure 7: Effect of pH on percentage rejection of Cr(VI) and fluoride for 5 ppm, 25 ppm and 100 ppm feed concentration at 10 bar applied pressure using the NF500 membrane.

proposes that the rejection of Cr(VI) and fluoride (solute) was enhanced with increasing pressure (see Figure 5). In size exclusion mechanism the pore size of the membrane and dimension of the solute play a significant part in finding the degree of separation. Negatively charged ions and a negatively charged membrane enhanced the Cr(VI) and fluoride rejection from binary solution due to the electrostatic charge repulsion mechanism.

4.4 pH effect on rejection

The pH effect on rejection of Cr(VI) and fluoride are mentioned in Figure 7. In the pH effect study, pH varied from 2, 4, 6, 8 and 10 which are in the working range of NF500 and the effect of pH on percent rejection with different feed concentrations (5, 25 and 100) of Cr(VI) and fluoride are studied. In an aqueous solution Cr(VI) can exist in various ionic forms ($HCrO_4^-$, CrO_4^{2-}, $Cr_2O_7^{2-}$) due to Cr(VI) concentration and solution pH. From Figure 7 we conclude that less rejection was observed in acidic conditions at pH 2 which appears due to the Donnan effect for the negatively charged membrane to have minor rejection to the monovalent anion $HCrO_4^-$. When the pH was set to 7 some of $HCrO_4^-$ anions converted in to CrO_4^{2-} and removal of was increased. When pH was adjusted to 8 and above, maximum rejection was observed. In case of fluoride the same trend has been found. Less rejection was found at pH 2 and higher rejection was observed at pH 8 and above. A similar effect of pH on the rejection of fluoride by the NF membrane was found in earlier reported studies (31, 47, 48). Hence, we can conclude that the NF500 membranes can work efficiently in the removal of Cr(VI) and fluoride when pH is adjusted above 8.0.

4.5 Investigation of MTPs and MTC

The MTC (k) and MTPs (σ and P_m) are simultaneously evaluated by using the CFSK model (with the help of the nonlinear parameter evaluation process) with given data of R_o and J_v at different pressures and constant feed rate by keeping the constant feed concentration. The MTC and MTPs of the NF500 membrane are shown in Table 2 where solute permeability P_m and reflection coefficient σ are dependent on the feed concentration. σ slightly decreases due to the reduction in solute rejection and P_m increases with feed concentration due to the high amount of solute passing through the membrane. The same kind of trend for NF membranes was observed by Murthy and co-workers (41, 42). The values of k shown in Table 2 are then used in Eq. [5] along with the previous data R_o and J_v to determine the true rejection R. Simultaneous observed rejection of Cr(VI) and fluoride by the NF500 membrane are compared with the true rejection estimated by the CFSK model are shown in Figure 8. Figure 8 indicates the good agreement for experimental rejection and true rejection for Cr(VI) and fluoride by the NF500 membrane.

5 Conclusion

The NF500 NF membrane was applied for simultaneous rejection of Cr(VI) and fluoride ions from a synthetic

Table 2: MTC and MTPs parameter estimated of NF500 membrane for removal Cr(VI) and F by the CFSK model.

Feed concentration (ppm)	Cr(VI)				Fluoride			
	Reflection coefficient σ	Solute permeability $P_m \times 10^5$ (cm/s)	Mass transfer coefficient $k \times 10^3$ (cm/s)	Root-MSE	Reflection coefficient σ	Solute permeability $P_m \times 10^5$ (cm/s)	Mass transfer coefficient $k \times 10^3$ (cm/s)	Root-MSE
5	0.9112	4.84	57.80	0.1712	0.8513	6.81	47.88	0.1478
10	0.8810	5.12	57.40	0.3301	0.8366	7.31	47.58	0.0814
25	0.8348	5.44	56.71	0.0410	0.8012	7.51	47.37	0.0340
50	0.7713	5.76	56.20	0.1547	0.7441	7.98	47.07	0.1044
100	0.7189	6.28	55.98	0.4102	0.6388	8.51	46.72	0.5011

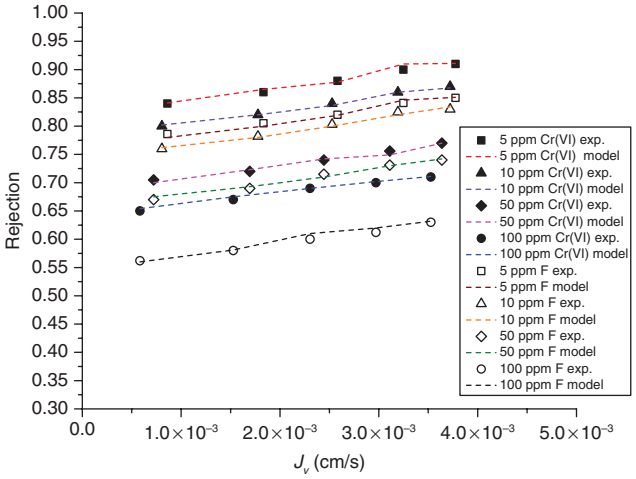

Figure 8: Experimental and estimated rejection of Cr(VI) and fluoride as a function of permeate flux.

binary solution with the study of various parameters: feed concentration, applied pressure, feed pH. The study concluded that Cr(VI) and fluoride rejection was enhanced with increasing applied pressure and decreased with the increase in feed concentration of Cr(VI) and fluoride. The pH study significantly effected the rejection of Cr(VI) and fluoride ions. The highest rejection was observed at pH 8 and above. MTC and MTPs estimation was done by using the CFSK model. Good agreement was found in experimental results and model predict results for simultaneous removal of Cr(VI) and fluoride.

Nomenclature

R	true solute rejection
k	mass transfer coefficient
R_o	observed solute rejection
J_v	permeate volume flux (m^3/m^2 s)
L_p	hydraulic permeability (m/s kPa)
P_m	overall solute permeability (m/s)
Δp	pressure difference across the membrane (kPa)

Greek symbols

σ	reflection coefficient
$\Delta\pi$	osmotic pressure difference across the membrane (kPa)

Acknowledgments: The authors are grateful to IIT Roorkee, India, for providing the facilities for this work. The authors would also like to thank the MHRD, Government of India for providing financial support.

References

1. Wahab Mohammad A, Othaman R, Hilal N. Potential use of nanofiltration membranes in treatment of industrial wastewater from Ni-P electroless plating. Desalination 2004;168:241–52.
2. Al-Rashdi B, Somerfield C, Hilal N. Heavy metals removal using adsorption and nanofiltration techniques. Sep Purif Rev. 2011;40:209–59.
3. Murthy ZVP, Gaikwad MS. Separation of praseodymium(III) from aqueous solutions by nanofiltration. Can Metall Q. 2013;52:18–22.
4. Murthy ZVP, Gaikwad MS. Preparation of chitosan-multiwalled carbon nanotubes blended membranes: characterization and performance in the separation of sodium and magnesium ions. Nanoscale Microscale Thermophys Eng. 2013;17:245–62.
5. Gzara L, Dhahbi M. Removal of chromate anions by micellar-enhanced ultrafiltration using cationic surfactants. Desalination 2001;137:241–50.
6. Cervantes C, Garcia JC, Devars S, Corona FG, Tavera HL, Carlos Torres-guzman J, Sanchez RM. Interactions of chromium with micro-organisms and plants. FEMS Microb Rev. 2001;25:335–47.
7. Visvanathan C, Ben Aim R, Vigneswaran S. Application of cross-flow electro-microfiltration in chromium wastewater treatment. Desalination 1989;71:265–76.
8. Galan B, Castaneda D, Ortiz I. Removal and recovery of Cr(VI) from polluted ground waters: A comparative study of ion-exchange technologies. Water Res. 2005;39:4317–324.
9. Basha S, Murthy ZVP, Jha B. Biosorption of hexavalent chromium by chemically modified seaweed, Cystoseira indica. Chem Eng J. 2008;137:480–88.

10. Basha S, Murthy ZVP. Kinetic and equilibrium models for biosorption of Cr(VI) on chemically modified seaweed, Cystoseira indica. Process Biochem. 2007;42:1521–9.
11. Ghiaci M, Kia R, Abbaspur A, Seyedeyn-Azad F. Adsorption of chromate by surfactant-modified zeolites and MCM-41 molecular sieve. Sep Purif Technol. 2004;40:285–95.
12. Kishore N, Sachan S, Rai KN, Kumar A. Synthesis and characterization of a nanofiltration carbon membrane derived from phenol-formaldehyde resin. Carbon 2003;41:2961–72.
13. Pugazhenthi G, Kumar A. Chromium(VI) separation from aqueous solution using anion exchange membrane. AIChE J. 2005;51:2001–10.
14. Chiha M, Samar MH, Hamdaoui O. Extraction of chromium(VI) from sulphuric acid aqueous solutions by a liquid surfactant membrane (LSM). Desalination 2006;194:69–80.
15. Liu M, Sun RY, Zhang JH, Bi NY, Wei L, Liu P, Kei CF. Elimination of excess fluoride in potable water with coarcervation by electrolysis using aluminium anode. Fluoride 1983;20:54–63.
16. Cheng LS. Electro-chemical method to remove fluoride from drinking water. Water Supply 1985;3:177–86.
17. Chaturvedi AK, Yadava KP, Pathak KC, Singh VN. Defluoridation of water by adsorption of fly ash. Water Air Soil Pollut. 1990;49:51–61.
18. Sujana MG, Thakur RS, Rao SB. Removal of fluoride from aqueous solution by using alum sludge. J Coll Interface Sci. 1998;206:94–101.
19. Toyoda A, Taira T. A new method for treating fluorine wastewater to reduce sludge and running costs. IEEE Trans Semiconductor Manuf. 2000;13:305–09.
20. Ganvir V, Das K. Removal of fluoride from drinking water using aluminum hydroxide coated rice husk ash. J Hazard Mater. 2011;185:1287–94.
21. Dou XM, Zhang YS, Wang HJ, Wang TJ, Wang YL. Performance of granular zirconium-iron oxide in the removal of fluoride from drinking water. Water Res. 2011;45:3571–8.
22. Poursaberi T, Hassanisadi M, Torkestani K, Zare M. Development of zirconium (IV)-metalloporphyrin grafted Fe_3O_4 nanoparticles for efficient fluoride removal. Chem Eng J. 2012;189:117–25.
23. Turner BD, Binning P, Stipp SLS. Fluoride removal by calcite: evidence for fluorite precipitation and surface adsorption. Environ Sci Technol. 2005;39:9561–8.
24. Sundaram CS, Meenakshi S. Fluoride sorption using organic-inorganic hybrid type ion exchangers. J Colloid Interf Sci. 2009;333:58–62.
25. Sahli MAM, Annouar S, Tahaikt M, Mountadar M, Souflane A, Elmidaoui A. Fluoride removal for underground brackish water by adsorption on the natural chitosan and by electrodialysis. Desalination 2007;212:37–45.
26. Maliyekkal SM, Sharma AK, Philip L. Manganese-oxide-coated alumina: a promising sorbent for defluoridation of water. Water Res. 2006;40:3497–506.
27. Gong WX, Qu JH, Liu RP, Lan HC, Adsorption of fluoride onto different types of aluminas. Chem Eng J. 2012;189:126–33.
28. Du DY, Yu ZS, Liu JZ, Lu XH. Adsorption of fluoride from aqueous solution by aluminum pillared rectorite. Fresen Environ Bull. 2005;14:972–5.
29. Smittakorn S, Jirawongboonrod N, Mongkolnchai-arunya S, Durnford D. Homemade bone charcoal adsorbent for defluoridation of groundwater in Thailand. J Water Health 2010;8:826–36.
30. Hu K, Dickson JM, Nanofiltration membrane performance on fluoride removal from water. J Membr Sci. 2006;279:529–38.
31. Richards LA, Vuachere M, Schafer AI. Impact of pH on the removal of fluoride, nitrate and boron by nanofiltration/reverse osmosis. Desalination 2010;261:331–7.
32. Hu CY, Lo SL, Kuan WH, Lee YD. Removal of fluoride from semiconductor wastewater by electrocoagulation–flotation. Water Res. 2005;39:895–901.
33. de Luna MDG, Warmadewanthi, Liu JC. Combined treatment of polishing wastewater and fluoride-containing wastewater from a semiconductor manufacturer. Colloids Surf A Physicochem Eng Aspects 2009;347:64–8.
34. Secco d'Aragona F. Dislocation etch for (100) planes in silicon. J Electrochem Soc. 1972;119;948–51.
35. Yang KH. An etch for delineation of defects in silicon. Electrochem Soc. 1984;131:1140–1145.
36. Aoudj S, Khelifa A, Drouiche N, Hecini M. HF wastewater remediation by electrocoagulation process. Desalination Water Treat. 2013;51:1596–602.
37. Aoudj S, Khelifa A, Drouiche N, Belkada R, Miroud D. Simultaneous removal of chromium(VI) and fluoride by electrocoagulation–electroflotation: application of a hybrid Fe-Al anode. Chem Eng J. 2015;267:153–62.
38. Clesceri LS, Greenberg EA, Eaton AD. Standard methods for the examination of water and wastewater. Washington: American Public Health Association; 1998.
39. Murthy ZVP, Gupta SK. Estimation of mass transfer coefficient using a combined nonlinear membrane transport and film theory model. Desalination 1997;109:39–49.
40. Spiegler K, Kedem O. Thermodynamics of hyperfiltration (reverse osmosis): criteria for efficient membranes. Desalination 1966;1:311–26.
41. Murthy ZVP, Chaudhari LB. Application of nanofiltration for the rejection of nickel ions from aqueous solutions and estimation of membrane transport parameters. J Hazard Mater 2008;160:70–7.
42. Murthy ZVP, Gupta SK. Thinfilm composite polyamide membrane parameters estimation for the phenol-water system by reverse osmosis. Sep Sci Technol. 1998;33:2541–57.
43. Vaidya SY, Simaria AV, Murthy ZVP. Reverse osmosis transport models evaluation: a new approach. Indian J Chem Technol. 2001;8:335–43.
44. Ballet GT, Gzara L, Hafiane A, Dhahbi M. Transport coefficients and cadmium salt rejection in nanofiltration membrane. Desalination 2004;167:369–76.
45. Mehiguene K, Garba Y, Taha S, Gondrexon N, Dorange G. Influence of operating conditions on the retention of copper and cadmium in aqueous solutions by nanofiltration: experimental results and modeling. Sep Purif Technol. 1999;15:181–7.
46. Kumar R, Bhakta P, Chakrabortty S, Pal P. Separating cyanide from coke wastewater by cross flow nanofiltration. Sep Sci Technol. 2011;46;2119–27.
47. Wei-fang MA, WEN-jun L, Guo-wei C. Factors influencing the removal of fluoride from groundwater by nanofiltration. Proc. ICBBE'09. International Conference on Bioinformatics and Biomedical Engineering, Beijing; 2009.
48. Chakrabortty S, Roy M, Pal P. Removal of fluoride from contaminated groundwater by cross flow nanofiltration: transport modeling and economic evaluation. Desalination 2013;313:115–24.